Nuclear Instruments and Methods in Physics Research A 850 (2017) 25–34

Contents lists available at ScienceDirect

Nuclear Instruments and Methods in Physics Research A

journal homepage: www.elsevier.com/locate/nima

Characterizing the behavior of scattered radiation in multi-energy x-ray imaging

Artur Sossin[a,*], V. Rebuffel[a], J. Tabary[a], J.M. Létang[b], N. Freud[b], L. Verger[a]

[a] *CEA-LETI MINATEC Grenoble, F-38054 Grenoble, France*
[b] *Univ Lyon, INSA-Lyon, Université Lyon 1, UJM-Saint Etienne, CNRS, Inserm, Centre Léon Bérard, CREATIS UMR 5220 U1206, F-69373 Lyon, France*

ARTICLE INFO

Keywords:
Multi-energy
X-ray scatter
Simulation
Experiments

ABSTRACT

Scattered radiation results in various undesirable effects in medical diagnostics, non-destructive testing (NDT) and security x-ray imaging. Despite numerous studies characterizing this phenomenon and its effects, the knowledge of its behavior in the energy domain remains limited. The present study aims at summarizing some key insights on scattered radiation originating from the inspected object. In addition, various simulations and experiments with limited collimation on both simplified and realistic phantoms were conducted in order to study scatter behavior in multi-energy x-ray imaging. Results showed that the spectrum shape of the scatter component can be considered preserved in the first approximation across the image plane for various acquisition geometries and phantoms. The variations exhibited by the scatter spectrum were below 10% for most examined cases. Furthermore, the corresponding spectrum shape proved to be also relatively invariant for different experimental angular projections of one of the examined phantoms. The observed property of scattered radiation can potentially lead to the decoupling of spatial and energy scatter components, which can in turn enable speed ups in scatter simulations and reduce the complexity of scatter correction.

1. Introduction

In medical diagnostics, non-destructive testing (NDT) and security x-ray imaging applications each detector pixel measures a sum of two signals: primary and scattered radiation (Fig. 1). The former consists of photons that have not been stopped or deviated by any interaction whilst the latter refers to signals measured by detector pixels due to the contribution of secondary photons, which are produced through Compton and Rayleigh interactions occurring in the object. Fluorescence radiation can also contribute in the case of high Z material presence in the inspected object and if the corresponding absorption edges are located within the energy range used for imaging.

Since the considered applications rely on the hypothesis that scatter radiation is absent in the acquisitions, the presence of the latter induces various undesirable effects in x-ray imaging such as bias, loss of spatial contrast and artifacts [1]. This is especially true for geometries with limited collimation. Thus, there is a great interest in studying the behavior of x-ray scatter, in order to provide some form of compensation of its effects in x-ray imaging. Moreover, with the emergence of multi-energy x-ray imaging, it also becomes important to examine scattered radiation in the energy domain.

In the present study the authors aim to provide a brief summary on existing observations with respect to x-ray scatter (Section 2) and to further characterize its behavior in energy-resolved x-ray imaging through simulations (Section 3) and experiments (Section 4).

2. Existing observations on the behavior of x-ray scatter

Unlike primary radiation, which can be described by direct analytical expressions, such as the Beer-Lambert (BL) law, scattered radiation does not have an equivalent expression. Although a buildup factor is sometimes used in the BL law, it is only a generalization of the complex probability models describing the photon scattering interactions. However, approximate models for first order scatter can still be found in the literature [2,3,4].

Regarding the nature of the effect, it is well known that x-ray scatter is object and geometry dependent [5]. For a fixed object-to-detector distance (ODD), also known as air gap, larger objects provide more scattered photons, as there is more material for the x-ray photons to interact with. This assumption is valid only if the object is entirely irradiated. Additionally, high Z materials (e.g. chrome) do not scatter as much as low Z materials (e.g. oxygen). Moreover, if one fixes the object and reduces the x-ray field until reaching a pencil beam (thus reducing the object fraction being irradiated), the scatter component

* Corresponding author.
E-mail address: artur.sossin@gmail.com (A. Sossin).

http://dx.doi.org/10.1016/j.nima.2017.01.032
Received 27 September 2016; Received in revised form 29 December 2016; Accepted 16 January 2017
Available online 18 January 2017
0168-9002/

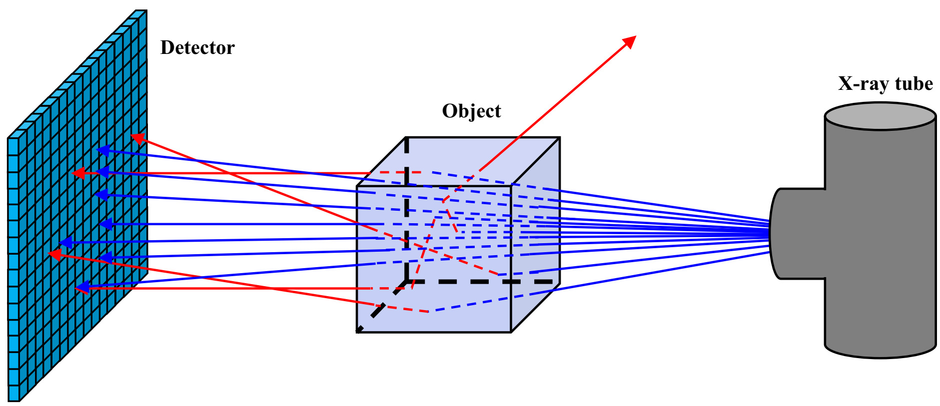

Fig. 1. Illustration of an x-ray acquisition system. Primary and scattered x-rays are marked blue and red respectively.

decreases to negligible amounts [6]. Finally, if for a fixed object the ODD is increased, scatter tends to reduce accordingly [5,7]. This is due to the fact that the solid angle covered by the detector reduces with respect to the scattering sources in the examined volume. Compared to computed tomography (CT) imaging, radiography usually uses larger field sizes and smaller ODDs. Thus, radiographic applications are likely to be more contaminated by scatter compared to CT imaging.

Another important observation concerns the spatial (function of detector pixel) behavior of x-ray scatter. More precisely, due to the randomness of interactions, the scatter spatial frequency is contained within the low frequency interval [8]. Although variations exist depending on the object and ODD, the spatial frequency of scatter remains sufficiently low to be represented by a sparse number of samples [9]. For example, it was reported through anthropomorphic phantom studies that, in diagnostic cone-beam CT (CBCT) with a source-to-axis distance (SAD) of 100 cm and an axis-to-detector distance (ADD) of 18–56 cm, the spatial scatter distribution can be sampled at rate as low as 5 cm^{-1} [9]. It is worth mentioning that the low spatial frequency scatter assumption is valid for a Compton interaction dominated scatter distribution (which is the most common case). However, in cases where Rayleigh scattering contribution is superior to that of Compton (e.g. after applying an anti-scatter grid), the spatial frequency tends to increase, due to the narrow angle forward directed nature of the respective interactions [5]. Moreover, in regions corresponding to object borders, the scatter distribution will exhibit higher frequency components (especially in NDT applications due to sharp object borders), which in turn may require an increased level of sampling [10].

With respect to CT, it was also found that x-ray scatter is a slowly varying distribution as a function of projection angle, and is thus contained within a low angular frequency interval [9]. This can also be linked to the high degree of randomness of scatter interactions in the object as well as to the slow change in ODD. The previously mentioned anthropomorphic phantom studies in CBCT (SAD and ADD of 100 cm and 18–56 cm, respectively) found that an angular sampling every 25° proves sufficient for adequately representing the respective scatter distribution [9].

Both observations are highly important for x-ray scatter simulation and correction as the low angular and spatial frequency assumption permits sub-sampling both spatially and angularly. In other words, for a complete x-ray CT acquisition, the scatter distribution can be highly accurately represented by a coarse grid of detector pixel measurements and sparse projections.

As for the behavior of scatter in the energy domain, some intuitive observations can already be made based on the underlying physical effects. Firstly, since Compton scattered photons contribute to the bulk of the scatter signal, the original x-ray spectrum will be shifted to the lower energies due to the energy shift experienced during this type of interaction. Several studies have confirmed this hypothesis [11,12,13]. However, if compared to the spatial domain characterization, the evaluation of the behavior of x-ray scatter in the energy domain still remains limited. The emergence of energy-resolved photon counting detectors for x-ray imaging adds motivation to the investigation of energetic properties of x-ray scatter.

As the amount of x-ray scatter is a geometrically dependent phenomenon and can thus result in varying level of image degradation, an indicator of the overall scatter amount must be defined. For this purpose, a metric known as the scatter-to-primary ratio (SPR) is often used [1]. It can be defined by the following expression:

$$SPR = \frac{I_S}{I_P} \times 100\%, \tag{1}$$

where I_S and I_P are the overall scatter and primary signal intensity, respectively, measured by the image receptor (or a certain region of interest).

3. Scatter behavior in the energy domain based on simulations

In order to perform x-ray scatter characterization in the energy domain, an analysis of various energy-resolved scatter images obtained with the aid of a recently developed simulation tool, Sindbad-SFFD [14], was conducted.

3.1. Acquisition configuration

The simulations were performed with a simplified numerical thorax phantom (Fig. 2) placed in a radiographic geometry with a varying air gap (Fig. 3). A tungsten anode (17°) x-ray tube was considered. The tube parameters were set to 110 kV with 0.25 cm of aluminum filtration. A point x-ray source was considered. In order to study the scatter signals due to purely photon-object interactions, a perfect (detector response not modeled) 512×512 pixel energy-resolved x-ray detector was used with a pixel size of 1 mm and energy bin width of 1 keV. In addition, photon noise was not included.

For each airgap the SPR was computed via (1) with the overall primary or scatter image intensities defined as follows:

$$\begin{aligned} I_P &= \textstyle\sum_{\mathbf{p},E} N_P(\mathbf{p}, E)\, E^* \\ I_S &= \textstyle\sum_{\mathbf{p},E} N_S(\mathbf{p}, E)\, E^* \end{aligned} \tag{2}$$

The quantities $\mathbf{p}=(x,y)$ and E in (2) represent a given image pixel and energy-resolved detector energy channel (bin) with median energy E^*, respectively. Additionally, $N_P(\mathbf{p}, E)$ and $N_S(\mathbf{p}, E)$ is the number of primary and scattered photons, respectively, measured in pixel $\mathbf{p}$ and energy bin E.